Diffusion and localization in quantum random resistor networks

Gerald Schubert and Holger Fehske
Institut für Physik, Ernst-Moritz-Arndt Universität Greifswald, 17487 Greifswald, Germany
(Received 2 July 2008; published 14 October 2008)

The theoretical description of transport in a wide class of novel materials is based upon quantum-percolation and related random-resistor-network (RRN) models. We examine the localization properties of electronic states of diverse two-dimensional quantum-percolation models using exact diagonalization in combination with kernel-polynomial-expansion techniques. Employing the local-distribution approach, we determine the arithmetically and geometrically averaged densities of states in order to distinguish extended, current-carrying states from localized ones. To get further insight into the nature of eigenstates of RRN models, we analyze the probability distribution of the local density of states in the whole parameter and energy range. For a recently proposed RRN representation of graphene sheets, we discuss leakage effects.

DOI: 10.1103/PhysRevB.78.155115 PACS number(s): 71.23.An, 71.30.+h, 05.60.Gg, 72.15.Rn

I. INTRODUCTION

Disorder is an intrinsic feature of many solid-state materials. The spatial inhomogeneity of a sample strongly affects the transport properties, particularly in low-dimensional systems where Anderson-localization effects play an important role.[1] Attempts to describe quantum transport in disordered media usually rely on free-electron models with random links between lattice sites and/or varying on-site potentials. Then transport is related to percolating-current patterns in a kind of random resistor network (RRN). RRN models apply to both classical- and quantum-percolation problems. For classical percolation the existence of a sample-spanning cluster ensures finite conductivity above a certain percolation threshold of accessible sites p_c. In the quantum case, the appearance of current-carrying states strongly depends on the (relative) importance of tunneling, scattering, and interference processes. For instance, strong scattering at the irregular boundaries of a conducting cluster may lead to a localization of the charge carrier even for $p > p_c$.

Over the past years percolation approaches have been employed in many circumstances, e.g., in order to model the transport properties of doped semiconductors[2] and granular metals,[3] the dynamics of atomic Fermi-Bose mixtures,[4] and the wave propagation through binary inhomogeneous media,[5] as well as the formation of novel two-dimensional (2D) spin liquids.[6] Another focal point is the metal-insulator transition, e.g., in 2D n-GaAs heterostructures[7] and colossal magnetoresistive manganite films,[8] or rather the superconductor-insulator and (integer) quantum Hall transitions.[9,10] Quite recently, the problem of disorder in systems with Dirac fermions has been studied in the context of dirty superconductors[11] and two-dimensional graphene.[12–15]

In mono- and bilayer graphene and graphene-based field-effect transistors, strong fluctuations in the local charge density and, thus, the local conductivity have been reported near the so-called neutrality point,[16–19] at which the conductivity reaches its minimum. The mesoscopic regions of different charge-carrier densities may be caused by inhomogeneities in the substrate or nonperfect stacking.[20–23] In order to model the minimal conductivity in graphene, a RRN representation of a graphene sheet was proposed by Cheianov *et al.*,[24] where random links between electron and hole "puddles" (corresponding to lattice sites) are assumed to determine the observable conductivity rather than the local conductivity of a puddle. Such a RRN formulated on a square lattice is closely related to a 2D quantum-percolation model with additional finite "leakage" between all lattice sites.

Motivated by this situation, in this paper we perform an in-depth numerical study of generalized 2D percolative RRN models. In particular we analyze how the leakage and connectivity rules influence the nature of the single-particle states. Since in two dimensions the problem of quantum percolation is still discussed controversially—especially with respect to the existence of a quantum-percolation threshold $p_c \leq p_q \leq 1$ (see, e.g., Refs. 25–36)—we rely on unbiased numerical techniques, which take quantum effects fully into account. To this end we employ the so-called local-distribution (LD) approach.[37,38] This technique, based on the determination of the distribution of the local density of states (LDOS) for all energies, has been previously applied in tackling localization phenomena in various disordered systems with great success.[39–46]

The paper is organized as follows. Section II introduces the RRN model and briefly outlines the LD approach. In Sec. III, we examine the localization properties of the eigenstates of RRN models by calculating the LDOS distribution, as well as the average and typical density of states. Section IV contains our conclusions.

II. MODEL AND METHODS

Let us consider a 2D square lattice with N sites on two sublattices α and β, which, e.g., might represent regions of different charge-carrier concentrations. The sublattices are linked by connection rules characteristic of specific materials. Generation rule A corresponds to a checkerboardlike structure (see upper left panel of Fig. 1). Regions (sites) of the sublattices are randomly connected with each other (lower panels of Fig. 1) according to the connection rules displayed in the upper right panel of Fig. 1. The hopping probability between such connected sites is assumed to be much higher than for hopping events to nearest neighbors. The latter ones are reduced by the leakage $\lambda < 1$.

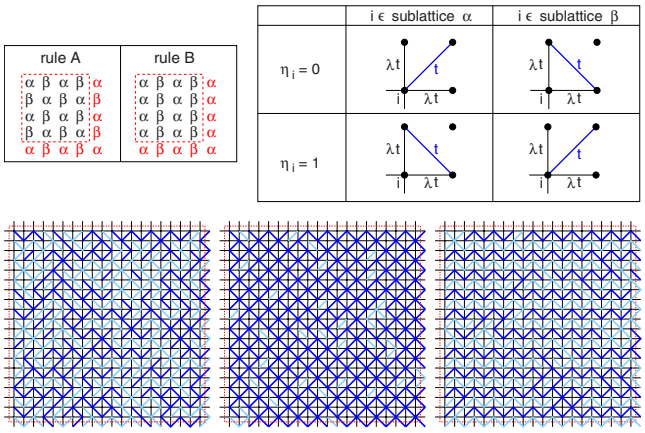

FIG. 1. (Color online) Upper left panel: Generation rules A and B for sublattices α and β. Upper right panel: Connection rules of neighboring sites on different sublattices. Lower panels: Three particular cluster realizations representing the above rules on a 20×20 lattice. From left to right: $p=0.50$, $p=0.90$ (rule A), and $p=0.90$ (rule B). Note that rules A and B become equivalent for $p=0.50$. At the red dashed lines the system is interconnected by periodic boundary conditions.

For the more abstract case of generation rule B (with the above connection rule), additional random bonds connect α to β sites, favoring the formation of quasi-one-dimensional zigzag chains. We still have a weak leakage between all neighboring sites. This generation rule can be interpreted as an attempt to incorporate a spatial anisotropy into the model.

In both cases, the corresponding RRN can be described by the Hamiltonian

$$H = -t\Bigg\{\sum_{i\in\alpha}[\eta_i c_i^\dagger c_{i+\nearrow} + (1-\eta_i)c_{i+\uparrow}^\dagger c_{i+\rightarrow}] + \sum_{i\in\beta}[\eta_i c_{i+\uparrow}^\dagger c_{i+\rightarrow} + (1-\eta_i)c_i^\dagger c_{i+\nearrow}] + \lambda\sum_i (c_i^\dagger c_{i+\rightarrow} c_i^\dagger c_{i+\uparrow})\Bigg\} + \text{H.c.} \quad (1)$$

Here $c_i^\dagger$ (c_i) creates (annihilates) an electron at site i and the arrows denote the nearest-neighbor sites of i in the corresponding direction. The discrete random variables $\eta_i \in \{0,1\}$ determine which diagonal in the plaquette is connected (cf. upper right panel of Fig. 1). By fixing the expectation value of the $\{\eta_i\}$ distribution, $p=\langle\eta_i\rangle$, we can control the sizes of the regions of connected lattice sites. For $p=0.5$ RRN model (1) does not depend on the generation rule A or B because of the symmetry of the bimodal $\{\eta_i\}$ distribution. In the limit of vanishing leakage we obtain the standard 2D quantum-percolation model using generation rule A.

To characterize the transport behavior of our model, we adopt the local-distribution approach. (For a detailed description of this technique, we refer the reader to Ref. 47 and references therein.) The main idea is to calculate the LDOS for all lattice sites i,

$$\rho_i(E) = \sum_{n=1}^{N} |\langle i|n\rangle|^2 \delta(E-E_n). \quad (2)$$

This quantity depends on the energy and varies from site to site. Moreover the ρ_i are specific for a particular sample (realization $\{\eta_i\}$). Calculating and recording ρ_i for many sites and realizations, we obtain the probability distribution $f[\rho_i]$ and distribution function

$$F[\rho_i] = \int_0^{\rho_i} f[\rho_i']d\rho_i' \quad (3)$$

of $\{\rho_i\}$. Both $f[\rho_i]$ and $F[\rho_i]$ are self-averaging. That is, in the thermodynamic limit, they are independent of the actual realization $\{\eta_i\}$ and the chosen sites $\{i\}$, but will be solely determined by the (global) model parameters p and λ and the generation rule. This restores translational invariance on the level of distributions.

A well-established criterion for localization then can be deduced from the shape of the distribution function. Since for an extended (current-carrying) state the amplitude of the wave function is more or less uniform, $F[\rho_i]$ steeply rises in the vicinity of the mean value of the LDOS, $\rho_{\text{me}}=\langle\rho_i\rangle$. For localized states, on the other hand, the LDOS strongly fluctuates throughout the lattice, leading to a rather gradual increase in $F[\rho_i]$ as a function of the magnitude of ρ_i. To capture this different behavior quantitatively, we may compare the arithmetic mean of the LDOS, ρ_{me}, to its geometric mean, the so-called typical DOS, $\rho_{\text{ty}}=e^{\langle\ln(\rho_i)\rangle}$; see, e.g., Ref. 39.

For extended states ρ_{me} and ρ_{ty} are of the same order, whereas ρ_{ty} vanishes for a localized state (or, in a finite system, is at least considerably suppressed). Of course, a reliable distinction between extended and localized states requires the consideration of different system sizes. For extended states $F[\rho_i]$ is independent of N. In contrast, for localized states $F[\rho_i]$ shifts toward lower values as N increases (causing the reduced value of ρ_{ty}).

The LDOS can be calculated very efficiently by means of the kernel-polynomial method (KPM).[48] Within this technique, the spectrum of H is expanded into a finite series of Chebyshev polynomials with additional damping factors. This approximation can be viewed as a convolution of the spectrum with the Jackson kernel, an almost Gaussian of width σ. As σ depends on the order of the Chebyshev series as well as on the energy, we have to adapt the expansion order to ensure a uniform resolution (constant σ) for the whole spectrum.[47]

III. RESULTS

In Fig. 2 we compare the mean and typical DOSs in dependence on λ and p for generation rules A and B. While the 2D percolation model ($\lambda=0$, rule A) exhibits symmetric DOS spectra, the inclusion of next-nearest-neighbor hopping causes an asymmetry that grows with increasing λ. Moreover, if $p>0.5$, the results obtained for the two generation rules differ significantly. For the A case the mean DOS resembles the 2D DOS. Generation rule B leads to a spectrum

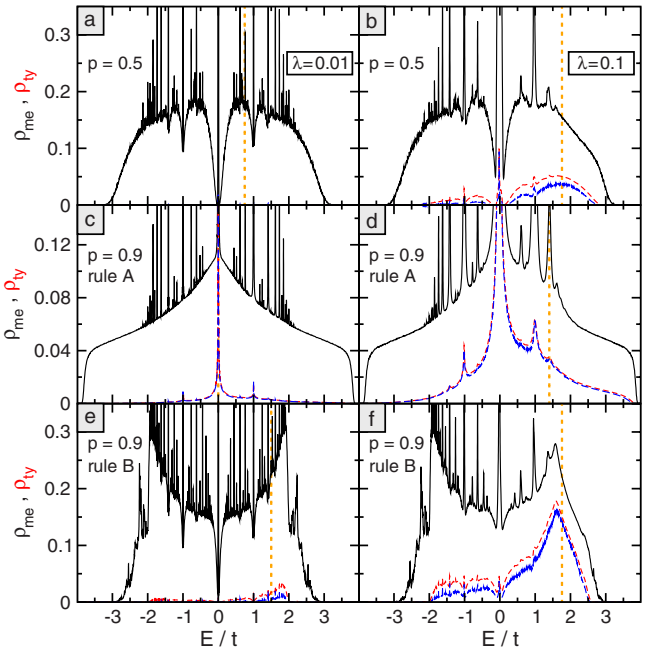

FIG. 2. (Color online) Mean (upper solid lines) and typical (lower dashed lines) DOSs. Results are shown for $N=400^2$ and $N\sigma=45$ for different p and λ and generation rules A and B. To illustrate the finite-size dependence of ρ_{ty}, the results for an $N=800^2$ lattice are included (long-dashed lines). The data are based on 10^5 (10^4) individual LDOS spectra for $N=400^2$ (800^2). Dotted vertical lines indicate the energies for which the distribution functions of the LDOS are given in Fig. 3.

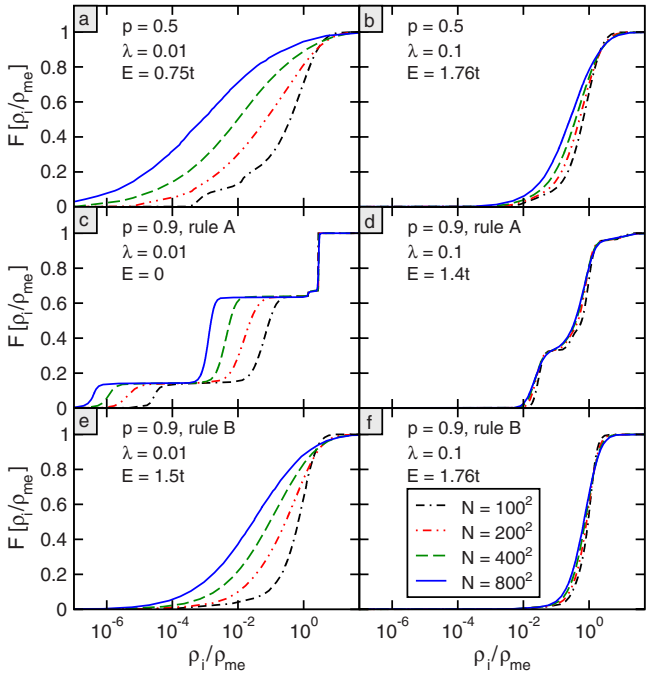

FIG. 3. (Color online) Distribution functions of the normalized LDOSs for the energies indicated by vertical lines in Fig. 2. The statistics is based on 10^7, 10^6, 10^5, and 10^4 LDOS values for $N=100^2$, 200^2, 400^2, and 800^2 and resolution $N\sigma=45$.

evocative of the DOS in one dimension. In both cases a multitude of spikes exist which we can attribute to localized states on "isolated" islands. This feature is well known from the binary-alloy model.[49] Increasing the leakage broadens the peaks and reduces their abundance because the isolation of the islands is weakened. Furthermore, the leakage shifts the "special energies" at which these peaks appear toward lower values as compared to those in the standard 2D percolation model.[49]

The typical DOS underlines the prominent role of the leakage. In Fig. 2(a) a vanishing ρ_{ty} suggests that all states are localized. As long as the leakage is very small, the typical DOS remains small as well throughout the band. This also holds for larger p and both generation rules. Sizable values of ρ_{ty} appear at larger values of λ only (compare the data for $\lambda=0.01$ and 0.1). As for the mean DOS, we observe a pronounced asymmetry of ρ_{ty} in the electronic band. This favors a finite typical DOS, i.e., extended states, for $E>0$. However, this has to be taken with caution. If we increase the system size together with the resolution of the KPM in such a way that the number of states within the width of the Jackson kernel, $N\sigma$, is kept constant, the picture changes. While for truly extended states ρ_{ty} should be independent of the system size [cf. Fig. 2(d)], in Figs. 2(b) and 2(f) the typical DOS decreases with increasing system size. This points toward a large localization length. While for small and moderate N the state still spans the entire lattice, the system size exceeds the localization length for larger N. Therefore, on a considerable number of sites the LDOS is very small, leading to a reduced value of ρ_{ty}. Then the question arises as to why in Fig. 2(d) the typical DOS is reduced as compared to ρ_{me}, even though this ratio is independent of N. This can be easily understood if we consider a perfectly ordered system, i.e., $p=1$. There the sites which do not belong to the spanning sublattice are also taken into account and amount to half of the lattice sites. In the absence of leakage, at those sites the LDOS vanishes and probing such a site completely suppresses ρ_{ty}. For finite λ, however, these sites have small amplitudes and in this manner ρ_{ty} is reduced as compared to ρ_{me} but is finite. These arguments also hold for Fig. 2(b), but there the low leakage suppresses the typical DOS almost completely, except for $E=0$.

As mentioned above, the comparison of ρ_{ty} and ρ_{me} may only serve as a first indication of localization. A careful finite-size scaling of the full probability function (or the distribution function) of the LDOS allows for a more reliable distinction between extended and localized states.

Thereto, in Fig. 3 we show for the same sets of parameters the distribution function of the LDOS at various characteristic energies. In the panels of Fig. 2 these energies are indicated by vertical dotted lines.

Here one crucial point concerns the normalization of ρ_i to ρ_{me}. For a completely extended state, with uniform amplitudes, the distribution function would be a step function. Due to the used scaling, this step would be located at $\rho_i/\rho_{me}=1$, irrespective of the system size. The random structure of the underlying lattice will distort this perfect jumplike behavior of $F[\rho_i/\rho_{me}]$. Nevertheless extended states are characterized by an N-independent distribution function [cf. Fig. 3(d)]. In contrast, for localized states, $F[\rho_i/\rho_{me}]$ constantly shifts toward lower values as N increases [cf. Figs. 3(a) and 3(e)].

Depending on the localization length, this effect is more or less pronounced. Thus, a wide range of system sizes is necessary in order to discriminate localized from extended states by means of finite-size scaling [cf. Figs. 3(b) and 3(f)].

A particular interesting shape of $F[\rho_i/\rho_{\mathrm{me}}]$ appears in Fig. 3(c), for a state in the band center. From the multistep structure, we may deduce that the probability distribution is mainly concentrated around three values. The largest of those values is independent of N, while the others show the above discussed variation. This behavior can be explained by considering again the completely ordered case. In the absence of leakage the $E=0$ eigenstate is highly degenerate: we have $N/2$ completely localized states, one on each isolated site. The other half of the eigenstates are extended in the perfect lattice, providing energies in the whole band. As the LDOS probes the complete eigenspace and not just the amplitude of one particular eigenstate, at $E=0$ we obtain the same value of $\rho_i/\rho_{\mathrm{me}}$ for each isolated site. Introducing a small leakage kills the high degeneracy in principle. Due to the finite-energy resolution of the KPM, however, still many of these states contribute to the LDOS at $E=0$. In the presence of imperfections ($p<1$), some of the former isolated sites will now be connected to form larger islands. Then less than $N/2$ states will contribute to the isolated islands' peak at high $\rho_i/\rho_{\mathrm{me}}$ [but still around 38% in Fig. 3(c)]. The second step, having a weight of about 50%, is due to sites on the highly connected majority sublattice, on which the LDOS is reduced but finite due to the leakage. The remaining lowest step originates from more complicated islands of several sites. On those islands (two, three, and so on sites), the $E=0$ eigenstates have vanishing amplitudes on some sites. Due to the leakage these sites again acquire a finite value of ρ_i.

To get additional insight into the spatial structure of the eigenstates, we investigate a smaller 128×128 system using exact-diagonalization techniques. Figure 4 visualizes characteristic eigenstates for the parameters discussed in Figs. 2 and 3. Most notable is the pronounced leakage dependence of the results. While we see clear localization for $\lambda=0.01$ [Figs. 4(a) and 4(e)], in the high-leakage case all states span the entire lattice. The one-dimensional (1D) structure for rule B and large p, which we already found in the DOS in Fig. 2(e), is also predominant in Fig. 4(e). In Fig. 4(c), notably in the magnifying inset, we see our assumption confirmed, that sites with large amplitudes are almost exclusively isolated, with the exception of some larger islands. Having the sharp step in mind, which occurs in Fig. 3(c) at large $\rho_i/\rho_{\mathrm{me}}$, the alert reader may wonder about the different amplitudes in Fig. 4(c) and the rather smooth increase in $F[N|\langle i|n\rangle|^2]$ in the middle column. This discrepancy is again due to the high degeneracy of the $E=0$ state and the fact that the LDOS takes into account the whole $E=0$ eigenspace. In contrast, for $N|\langle i|n\rangle|^2$, we randomly pick one particular eigenstate out of this subspace. For the other $E=0$ eigenstates, $F[N|\langle i|n\rangle|^2]$ looks similar; only the location of the sites with maximum amplitudes differ. Clearly, the physically relevant quantity is the LDOS, as the choice of eigenvectors which span the eigenspace is arbitrary up to any linear combinations of them. Summing up all eigenstates to $E=0$ for a fixed lattice site, we indeed get the same amplitude on each isolated site, which brings us back to the findings in Fig. 3(c). Finally we

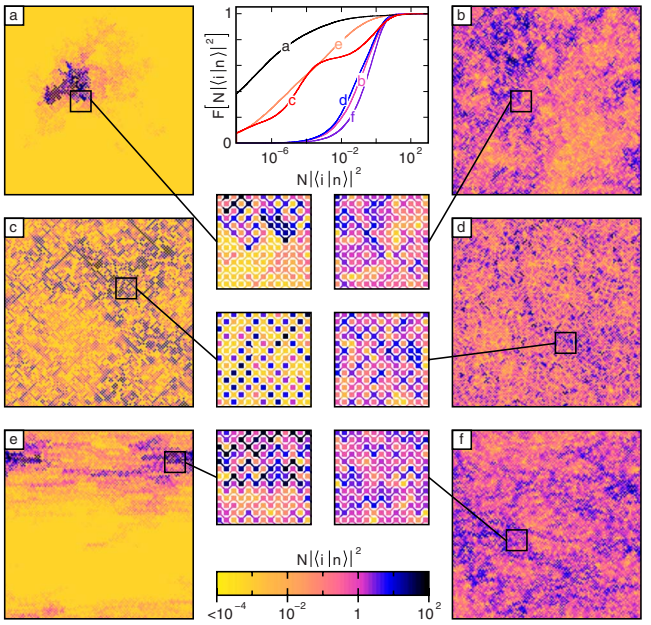

FIG. 4. (Color online) Normalized occupation probabilities $N|\langle i|n\rangle|^2$ of several characteristic eigenstates $|n\rangle$ on a $N=128^2$ lattice. The generation rules, doping, and leakage as well as the chosen energies E_n correspond to the ones for which the distribution functions of the LDOS has been presented in Fig. 3 (same order of panels). In the center column the distribution function of the normalized occupation probability is shown for these states. Furthermore, for each state an enlargement of a characteristic region together with the local structure of the present links is shown.

consider the case of higher leakage ($\lambda=0.1$), where all states look rather similar. Here the amplitudes fluctuate over a smaller range, and the fluctuations occur on very short spatial scales. This is most pronounced in Figs. 4(d) and 4(f) where no global structures can be distinguished, in accordance with the notion of extended states. In contrast, although the state in Fig. 4(b) spans the entire lattice, we observe sizable regions with higher and lower amplitudes than the mean value. Presumably, these inhomogeneities are even more pronounced for larger systems which, however, (as yet) are not accessible by our exact-diagonalization studies. In any case, the shifting of the LDOS distribution function in Fig. 3(b) suggests this state to be localized on large length scales.

IV. SUMMARY

In this work we investigated the two-dimensional quantum-percolation problem for a broader class of random-resistor-network models including leakage terms. Combining exact diagonalization, Chebyshev expansion, and local-distribution approaches in calculating the local density of states, we determine—after a careful finite-size scaling—the localization properties of the single-particle eigenstates. We found that current-carrying states exist and that the appearance of diffusion is mainly triggered by the amount of leakage. In contrast to previous work we analyzed the nature of the single-particle states in the whole energy band and not

just the vicinity of the neutrality point in the band center $E=0$. A tendency toward extended states is observed for $E>0$. In view of the simplicity of the considered RRN model, our data are certainly not yet suited to be compared against real transport data for, e.g., undoped graphene monolayers. Nevertheless, using unbiased numerics on a microscopic level, we fully account for quantum effects in a RRN model originally designed to describe transport in a graphene-based field-effect transistor, and we received results that support a minimal conductivity in graphene.

ACKNOWLEDGMENTS

The numerical calculations were performed on the HLRB at LRZ Munich and the TeraFlop compute cluster at the Institute of Physics, Greifswald University.

[1] P. W. Anderson, Phys. Rev. **109**, 1492 (1958).
[2] M. Inui, S. A. Trugman, and E. Abrahams, Phys. Rev. B **49**, 3190 (1994).
[3] M. V. Feigel'man, A. S. Ioselevich, and M. A. Skvortsov, Phys. Rev. Lett. **93**, 136403 (2004).
[4] A. Sanpera, A. Kantian, L. Sanchez-Palencia, J. Zakrzewski, and M. Lewenstein, Phys. Rev. Lett. **93**, 040401 (2004).
[5] Y. Avishai and J. Luck, Phys. Rev. B **45**, 1074 (1992).
[6] R. Yu, T. Roscilde, and S. Haas, Phys. Rev. Lett. **94**, 197204 (2005).
[7] S. Das Sarma, M. P. Lilly, E. H. Hwang, L. N. Pfeiffer, K. W. West, and J. L. Reno, Phys. Rev. Lett. **94**, 136401 (2005).
[8] T. Becker, C. Streng, Y. Luo, V. Moshnyaga, B. Damaschke, N. Shannon, and K. Samwer, Phys. Rev. Lett. **89**, 237203 (2002).
[9] Y. Dubi, Y. Meir, and Y. Avishai, Phys. Rev. B **71**, 125311 (2005).
[10] N. Sandler, H. R. Maei, and J. Kondev, Phys. Rev. B **70**, 045309 (2004).
[11] P. J. Hirschfeld and W. A. Atkinson, J. Low Temp. Phys. **126**, 881 (2002).
[12] V. M. Pereira, F. Guinea, J. M. B. Lopes dos Santos, N. M. R. Peres, and A. H. Castro Neto, Phys. Rev. Lett. **96**, 036801 (2006).
[13] I. Martin and Y. M. Blanter, arXiv:0705.0532 (unpublished).
[14] S.-J. Xiong and Y. Xiong, Phys. Rev. B **76**, 214204 (2007).
[15] A. Rycerz, J. Tworzydło, and C. W. J. Beenakker, Europhys. Lett. **79**, 57003 (2007).
[16] K. S. Novoselov, E. McCann, S. V. Morozov, V. I. Fal'ko, M. I. Katsnelson, U. Zeitler, D. Jiang, F. Schedin, and A. K. Geim, Nat. Phys. **2**, 177 (2006).
[17] S. Cho and M. S. Fuhrer, Phys. Rev. B **77**, 081402(R) (2008).
[18] J. Martin, N. Akerman, G. Ulbricht, T. Lohmann, J. H. Smet, K. von Klitzing, and A. Yacoby, Nat. Phys. **4**, 144 (2008).
[19] M. I. Katsnelson, K. S. Novoselov, and A. K. Geim, Nat. Phys. **2**, 620 (2006).
[20] E. Rossi and S. Das Sarma, arXiv:0803.0963, Phys. Rev. Lett. (to be published).
[21] Y.-W. Tan, Y. Zhang, K. Bolotin, Y. Zhao, S. Adam, E. H. Hwang, S. Das Sarma, H. L. Stormer, and P. Kim, Phys. Rev. Lett. **99**, 246803 (2007).
[22] J. H. Chen, C. Jang, M. S. Fuhrer, E. D. Williams, and M. Ishigami, Nat. Phys. **4**, 377 (2008).
[23] M. I. Katsnelson and A. K. Geim, Philos. Trans. R. Soc. London, Ser. A **366**, 195 (2008).
[24] V. V. Cheianov, V. I. Fal'ko, B. L. Altshuler, and I. L. Aleiner, Phys. Rev. Lett. **99**, 176801 (2007).
[25] G. Schubert and H. Fehske, Phys. Rev. B **77**, 245130 (2008).
[26] C. M. Soukoulis and G. S. Grest, Phys. Rev. B **44**, 4685 (1991).
[27] A. Mookerjee, I. Dasgupta, and T. Saha, Int. J. Mod. Phys. B **9**, 2989 (1995).
[28] A. Bunde, J. W. Kantelhardt, and L. Schweitzer, Ann. Phys. **7**, 372 (1998).
[29] G. Hałdas, A. Kolek, and A. W. Stadler, Phys. Status Solidi B **230**, 249 (2002).
[30] T. Odagaki and K. C. Chang, Phys. Rev. B **30**, 1612 (1984).
[31] V. Srivastava and M. Chaturvedi, Phys. Rev. B **30**, 2238 (1984).
[32] M. Letz and K. Ziegler, Philos. Mag. B **79**, 491 (1999).
[33] D. Daboul, I. Chang, and A. Aharony, Eur. Phys. J. B **16**, 303 (2000).
[34] A. Eilmes, R. A. Römer, and M. Schreiber, Physica B **296**, 46 (2001).
[35] H. N. Nazareno, P. E. de Brito, and E. S. Rodrigues, Phys. Rev. B **66**, 012205 (2002).
[36] M. F. Islam and H. Nakanishi, Phys. Rev. E **77**, 061109 (2008).
[37] A. Alvermann and H. Fehske, J. Phys.: Conf. Ser. **35**, 145 (2006).
[38] A. Alvermann and H. Fehske, Lect. Notes Phys. **739**, 505 (2008).
[39] G. Schubert, A. Weiße, G. Wellein, and H. Fehske, in *High Performance Computing in Science and Engineering, Garching 2004*, edited by A. Bode and F. Durst (Springer-Verlag, Heidelberg, 2005), pp. 237–250.
[40] V. Dobrosavljević, A. A. Pastor, and B. K. Nikolić, Europhys. Lett. **62**, 76 (2003).
[41] A. Alvermann, G. Schubert, A. Weiße, F. X. Bronold, and H. Fehske, Physica B **359-361**, 789 (2005).
[42] G. Schubert, A. Weiße, and H. Fehske, Physica B **359-361**, 801 (2005).
[43] V. Dobrosavljević and G. Kotliar, Phys. Rev. Lett. **78**, 3943 (1997).
[44] K. Byczuk, W. Hofstetter, and D. Vollhardt, Phys. Rev. Lett. **94**, 056404 (2005).
[45] F. X. Bronold and H. Fehske, Phys. Rev. B **66**, 073102 (2002).
[46] F. X. Bronold, A. Alvermann, and H. Fehske, Philos. Mag. **84**, 673 (2004).
[47] G. Schubert and H. Fehske, Lect. Notes Phys. (to be published).
[48] A. Weiße, G. Wellein, A. Alvermann, and H. Fehske, Rev. Mod. Phys. **78**, 275 (2006).
[49] G. Schubert, A. Weiße, and H. Fehske, Phys. Rev. B **71**, 045126 (2005).